ELSEVIER

Journal of Food Engineering **37** (1998) 127–141
© 1998 Elsevier Science Limited. All rights reserved
Printed in Great Britain
PII: S0260-8774(98)00088-0 0260-8774/98 $19.00+0.00

Prediction of Chilling Times of Foods in Situations Where Evaporative Cooling is Significant—Part 2. Experimental Testing

Sawitri Chuntranuluck,[a] C. M. Wells[b] & A. C. Cleland[c]*

[a]Biotechnology Department, Kasetsart University, Bangkok 10900, Thailand
[b]Agriculture New Zealand Ltd, PO Box 8640, Christchurch, New Zealand
[c]College of Sciences, Massey University, Private Bag 11-222, Palmerston North, New Zealand

(Received 22 September 1997; accepted 26 May 1998)

ABSTRACT

The algebraic model developed in Part 1 for prediction of chilling times, where cooling at the product surface is by evaporation as well as convection, was tested. Experimental measurements were made by chilling cylindrical test samples constructed of a food analogue in an air chiller. During chilling, the surface of each sample was continually wetted by a wetting agent of known water activity and the relative humidity of the air was controlled. Over the 30 trials, the proposed method predicted measured equilibrium temperature, intercept and slope parameters of semi-log unaccomplished temperature change vs time plots as accurately as could reasonably be expected taking into account data uncertainties (agreement largely within ±6%, but at worst ±10%). Chilling times were also predicted sufficiently accurately for many industrial applications. The simple model can be used with confidence for most chilling conditions likely to be encountered in industrial practice and including a_w values below 1.0. Part 3 considers applications to food materials in which surface water activity may not be constant. *© 1998 Elsevier Science Limited. All rights reserved*

NOMENCLATURE

a_w	Water activity at product surface
Bi	Biot number ($h\,R\,k^{-1}$)

*Author to whom correspondence should be addressed.

c	Specific heat capacity (J kg^{-1} K^{-1})
f	Slope of a plot of ln Y vs Fo
E	Shape parameter; = 0.75 (infinite slab); = 1.76 (infinite cylinder); = 3 (sphere)
Fo	Fourier number ($k\ t\ \rho^{-1}\ c_p^{-1}\ R^{-2}$)
h	Surface heat transfer coefficient (W m^{-2} K^{-1})
H	Humidity ratio
j	Lag factor or intercept of a plot of ln Y vs Fo
k	Thermal conductivity (W m^{-1} K^{-1})
K	Mass transfer coefficient (kg s^{-1} m^{-2} Pa^{-1})
n	Shape parameter; = 1 (infinite slab); = 2 (infinite cylinder); = 3 (sphere)
p	Partial pressure of water vapour in air (Pa)
P	Total air pressure (Pa)
R	Characteristic length (radius) of product (m)
t	Time (s)
T	Temperature (K or °C)
v	Velocity (m s^{-1})
Y	Dimensionless temperature
ε	Latent heat of vaporisation of water (J kg^{-1})
ρ	Density of product (kg m^{-3})

Subscripts

a	Air
av	Mass-average
c	Centre
Conv	Convection only
eq	Equilibrium
Evap	Evaporation and convection
in	Initial
p	Product
r	Relative (humidity)
w	Saturation

INTRODUCTION

Air chilling of many unwrapped food products involves surface heat transfer by both convection and evaporation. The evaporative cooling effect can significantly change the rate of cooling compared with that which would arise if only convection was occurring. In Part 1, Chuntranuluck *et al.* (1998a) surveyed available chilling time prediction methods for such situations. They concluded that the theoretical accuracy of numerical methods solving the fundamental heat and mass transfer equations was almost impossible to realise in industrial practice because detailed data for mass transfer parameters were required, and these data were rarely available. They also found that most prediction methods had been derived by not attempting to model the mass transfer within the product at all, but instead assuming that its effect was to create a constant surface water activity, a_w. However, it was usually assumed that $a_w = 1$. Chuntranuluck *et al.* (1998a) proposed a new simple prediction method

requiring only algebraic calculation, but allowing $a_w \leq 1$, thus distinguishing it from previous methods. The method was derived by curve-fitting of finite difference predictions of chilling rates for infinite slabs, infinite cylinders and spheres across wide ranges of conditions. In making predictions, as well as the data that would normally be required to predict a convection-only chilling process, only two new data are required — a_w and H_r.

The first stage is to use the analytical solutions for chilling with convection only at the boundary, as conveniently stated by Cleland (1990), to find the appropriate slope and intercept parameters for convection only (f_{Conv}, j_{avConv} and j_{cConv}), which fit the one term approximation to the analytical solutions:

$$Y = \frac{(T - T_a)}{(T_{in} - T_a)} \approx j_{Conv}\, e^{-\beta^2(kt/\rho c_p R^2)} \approx j_{Conv} e^{-f_{Conv} Fo} \tag{1}$$

Equations (2)–(5) are then used to determine the slope and intercept parameters for cooling with evaporation and convection (f_{Evap}, j_{avEvap}, and j_{cEvap}):

$$\frac{f_{Evap}}{f_{Conv}} = 1 + \frac{Bi}{15(Bi^{1.5} + 1.5)} + \frac{T_a(H_r + 0.34) + (5H_r + 0.12T_{in} + 9.87)a_w^{0.8}}{19(Bi^{1.2} + 1.2)} \tag{2}$$

$$\begin{aligned} \frac{j_{cEvap}}{j_{cConv}} = 1 &- \frac{0.0153a_w^{2.4}}{Bi^{0.4}} + 0.0335\left(\frac{Bi^{4/3} + 1.85}{Bi^{4/3}/E + 1.85/n}\right)e^{-(Bi-2.5)^2} \\ &+ 0.0725H_r e^{-(Bi-0.7)^2} + T_a(0.00338H_r + 0.00413e^{-(Bi-0.9)^2}) \\ &- T_{in}(0.00447e^{-1.33Bi} + 0.000599) \end{aligned} \tag{3}$$

$$\frac{j_{avEvap}}{j_{avConv}} = 1 + \frac{(0.0345H_r + 0.00207(T_a - T_{in}) - 0.0228a_w^4)}{Bi^{0.333}}$$

$$-0.0321H_r e^{-(Bi-2.5)^2} - \left[0.00169T_a + 0.0166\left(\frac{Bi^{4/3} + 1.85}{Bi^{4/3}/E + 1.85/n}\right)\right]e^{-(0.1Bi)^2} \tag{4}$$

The product equilibrium temperature as $t \to \infty$ is defined as:

$$T_{eq} \approx T_a - \frac{18\varepsilon}{29c_a}\left(\frac{p_M - p_a}{P}\right) \approx T_a - \frac{18\varepsilon}{29c_a}\left(\frac{a_w p_{wM} - H_r p_{wa}}{P}\right) \tag{5}$$

Using convenient curve-fit equations for water thermophysical properties this can be restated as:

$$T_{eq} \approx T_a - \frac{18(2{\cdot}5 \times 10^6 - 2{\cdot}5 \times 10^3 T_{eq})}{29 c_a P} \times \{a_w \exp[23{\cdot}4759 - (3990{\cdot}56/T_{eq} + 233{\cdot}833)] - H_r \exp[23{\cdot}4759 - (3990{\cdot}56/T_a + 233{\cdot}833)]\} \quad (6)$$

Equation (6) can be solved iteratively, as T_{eq} is the only unknown, or alternatively Chuntranuluck (1995) presents some look-up charts for common ranges of T_a, a_w and H_r. The time to cool to a particular unaccomplished temperature ratio Y is then:

$$t = \left(\frac{\ln Y - \ln j_{Evap}}{f_{Evap}} \right) \frac{\rho c_p R^2}{k} \quad (7)$$

whereas the temperature at any time (as represented by Fo), is:

$$T = (T_{in} - T_{eq}) e^{(-f_{Evap} Fo + \ln j_{Evap})} + T_{eq} \quad (8)$$

Chuntranuluck *et al.* (1998a) presented statistics which showed that the proposed prediction method generally predicted chilling times within $\pm 5\%$ of the predictions made by the finite difference simulation. However, the ultimate proof of the accuracy of the method is determined by comparison with experimental data. In this extension to the theoretical work the methods used in, and results of the experimental testing for food analogue materials with constant surface water activity are reported. In Part 3, application of the method to real food materials is considered.

MATERIALS AND METHODS

Experimental design

Ideally, the experimental trials to ensure that the effects of evaporation are accurately predicted would be conducted across a wide range of likely practical chilling conditions defined by the five key variables a_w, H_r, T_{in}, T_a and Bi. A normal factorial design for five variables would be 32 runs, and these would only include two levels of each variable. In addition, there are three shapes to consider. To test the method at more levels of each variable a modified central composite design (including only two relative humidity levels, but three levels of the other variables), was used. Limitations in the equipment available prevented the use of more than two humidity levels. There were 30 runs using combinations of the following levels for each variable:

a_w	0.75, 0.88, 1.0
H_r	0.78, 0.91
T_{in} (°C)	20, 30, 40
T_a (°C)	0, 5, 10
Bi	0.9–1.0, 1.3–1.8, 3.5–4.1 (see below)

The theoretical testing had shown little difference in behaviour between the three shapes, and geometrically the cylinder is the 'middle' shape. For reasons of practicality to do with the equipment design, it was decided to carry out experiments with the infinite cylinder shape only.

Test objects and application of wetting agents

Aluminium cylindrical tubes of internal diameters 0.072 and 0.142 m were used. These were approximately 0.36 m in length. Polystyrene foam end caps were put on to ensure that heat transfer to the middle part of each cylinder was close to one-dimensionally axisymmetrical, according to the criteria of Cleland *et al.* (1994). The cylinders were filled with Tylose, a common food analogue material which has thermal properties similar to foods of about 75% water by composition (Riedel, 1960). The thermophysical properties of Tylose were recently measured by the Meat Industry Research Institute of New Zealand. Over the temperature range of interest mean values were $\rho c_p = 3.89 \times 10^6\ \mathrm{Jm^{-3}\,K^{-1}}$, $k = 0.500\ \mathrm{Wm^{-1}\,K^{-1}}$.

Two copper-constantan thermocouples were located on the central axis of each cylinder close to the mid-point height, each introduced from the opposite end. Two further thermocouples were placed on the inner surface at different locations around the cylindrical tube, but approximately at the mid-point height. The concept behind using aluminium was to confine the Tylose to the shape of a cylinder without introducing significant heat transfer resistance or significant extrathermal capacity.

To create a surface with a controlled and constant water activity, each cylinder was tightly wrapped in a single layer of a commercial cotton cloth. Due to unavailability of further supplies of the cloth used for the small cylinder at the time the larger cylinder size was made, the two cylinders were covered in different cloth. The cloth was kept fully wetted by supply of a wetting agent during each trial, thus creating a uniform water activity over the surface of each cylinder. To achieve three different levels of water activity three wetting agents were chosen—distilled water, a saturated sodium chloride solution, and a saturated potassium chloride solution. For the temperature range in use, the former saturated solution has a mean water activity of 0.75, and the latter 0.88. They are also relatively cheap and safe to use.

Reservoirs of each were prepared and, as shown in Fig. 1, during the course of each chilling trial a slow flow of the appropriate solution was fed by a small pump to a ring-shaped distributor at the top of each cylinder. From here it ran down to collect in a drain tray. As Fig. 2 shows, the starting temperature for the reservoir should be such that the reservoir cools at the same rate as the sample surface. This means that the flow of the wetting agent onto the surface is 'thermally neutral'. A number of trials were conducted in which the reservoir temperature was varied until the most appropriate starting temperature for each wetting agent was found. As thermal neutrality could not be exactly achieved, accurate setting of the wetting agent flowrate to minimise the wetting agent flow ensured that the extent of any heating or cooling by the wetting agent was small. This aspect is further discussed in the thesis on which this paper is based (Chuntranuluck, 1995).

Potassium chloride was the most difficult saturated salt solution to work with because it crystallised at lower temperature and damaged the feeding system. To avoid this problem, the feeding system had to be run at the same, or a little higher than, the temperature of the air. This meant that the addition of liquid to the

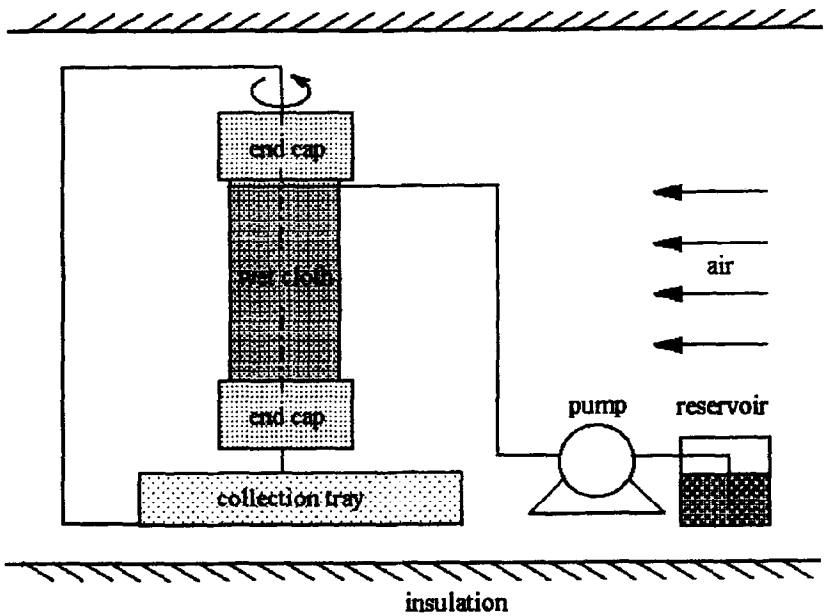

Fig. 1. Schematic diagram of the experimental apparatus installed in the air chiller showing both sample oscillation, and the supply system for wetting agent.

surface could have affected the cooling rate. Hence, there was more experimental error for runs with this salt solution.

Chilling tunnel

A locally designed and constructed pilot plant air chiller was available in which the air temperature could be set to temperatures in the range 0–10°C and controlled to ± 0.3°C. The chiller was arranged in a manner which produced a horizontal air flow through the section in which the test samples would be placed. Uniformity through this section was achieved by requiring the air flow to flow through a hole-plate distributor system. By use of fan control systems fitted to the chiller, three air velocities could be achieved—0.5, 1.1 and 3.4 m s^{-1}. Different *Bi* were thus obtained by varying cylinder size in combination with the different air velocities. Three *Bi* ranges, rather than three specific levels, were achieved.

Setting and control of relative humidity independently of air temperature and air velocity was difficult in this particular air chiller. Creation of a high relative humidity environment required increasing the refrigeration evaporator heat transfer surface area in use, and the addition of a wet heat source to the chiller. This typically gave a relative humidity of about 91%. Conversely, reducing the refrigeration heat transfer area, and adding a dry heat source to the chiller, allowed a level of 78% to be achieved. Chuntranuluck (1995) describes the methods used in more detail. For each run under different conditions considerable effort had to be made to reset all

the controls to regain stable operation and control, and ultimately this limited both the ranges of conditions available and the number of runs possible.

The test cylinders were mounted as shown in Fig. 1. The sample oscillator turned the cylinder to and fro through approximately 270° every 10 s. This helped ensure even surface heat transfer conditions on all parts of the cylinder surface.

Data acquisition systems

All temperatures were measured by 28–30 SWG copper–constantan thermocouples, referenced to an ice/water slurry as datum point. The millivolt readings created were transferred to an electronic data acquisition system (FIX™ supplied by Intellution Inc.). In this they were digitised and converted to temperature readings. The analogue to digital conversion system had a precision equivalent to ± 0.1°C, and tests of the thermocouples against the ice point reference suggested that the overall precision of temperature measurements was ± 0.2–0.3°C.

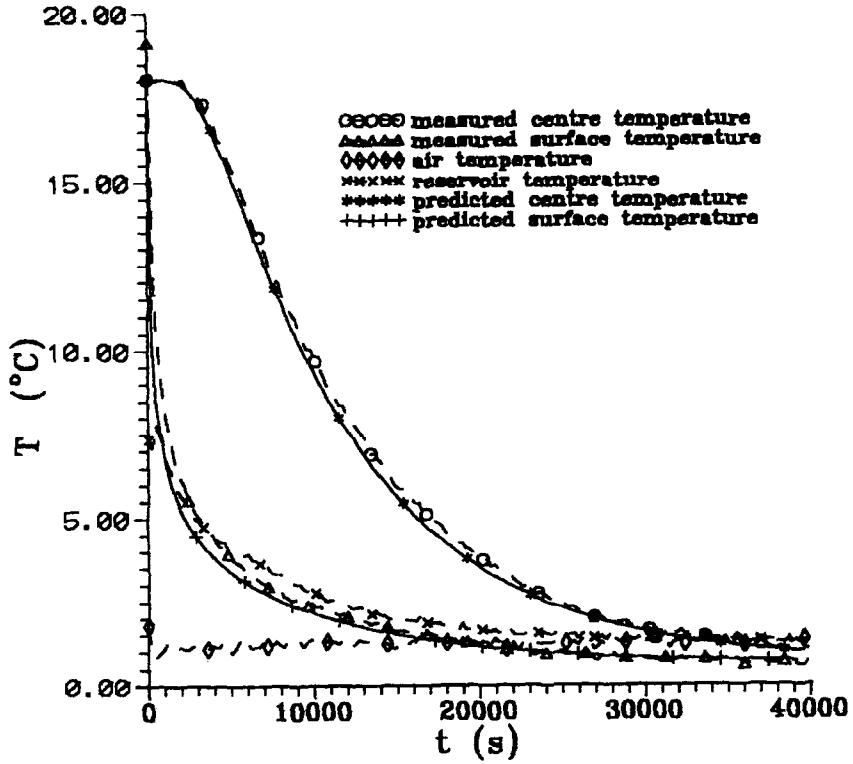

Fig. 2. Plot of sample temperature (°C) vs time (s) for chilling of the large cylinder in a run in which the wetting agent reservoir temperature was closely matched to the sample surface temperature. (Predictions shown are by the finite difference method of Chuntranuluck *et al.*, 1998a.)

Relative humidity was measured by a Michel Series 3000 dewpoint meter (for which the inaccuracy in dewpoint temperature translated to a potential relative humidity inaccuracy of $\pm 3\%$), and a Vaisala Humicap Type 1638 HM probe, both connected to the FIX data acquisition system. The latter is rated to $\pm 3\%$, and had been calibrated against a standard set of saturated salt solutions.

Air velocity was measured using a Dantec Low Velocity Transducer (Type 54R10) connected to a Dantec Low Velocity Flow Analyser (Type 54N10). This had been recently calibrated at a N.Z. Standards testing laboratory and its time-integrated mean velocity readings were considered accurate to $\pm 0.02\ \mathrm{m\ s^{-1}}$. A number of readings were taken around each cylinder while *in situ* within the air chiller, after the sample had equilibrated to the air temperature.

Experimental chilling method

Prior to the commencement of each experimental trial the test cylinder was placed in a warm room for sufficient time for it to equilibrate to room temperature. It was then insulated for transport to the chilling tunnel. Several hours prior to the start of a trial, the chilling tunnel was started and the controls hand-tuned to give stable operation at the required air temperature and relative humidity conditions. Once this was achieved, a reservoir of wetting agent was transferred to the tunnel, the insulated test sample was fully wetted with wetting agent at the warm room temperature and the sample transferred to beside the chilling tunnel. Thermocouples were connected to the data logger as rapidly as possible, and then the test sample transferred to the chilling tunnel, where the supply of the wetting agent was immediately started. Data were then logged over the run length, which was normally 10–15 h. Finally, air velocity data were recorded.

Heat transfer coefficients

Heat transfer coefficients (h) were determined by cooling the infinite cylinders in separate trials where the cloth was wetted but a thin plastic film covered the wet cloth to avoid evaporation. The analytical solution for heat conduction were used to back-calculate h values from the temperature–time data in such trials. It was considered that the heat transfer resistance of the thin plastic film was negligible.

RESULTS AND DISCUSSION

Heat transfer coefficients

The measured surface heat transfer coefficient represents the heat transfer resistance in the air boundary layer, and the resistance in the wetted cloth (the resistance of the aluminium was negligible). The boundary layer effects include both convective and radiation heat transfer at the product surface. Small differences between the two different cloth types, and between different wetting agents (due to their different thermal conductivities), were expected. Hence the heat transfer coefficent

was related to air velocity, and separately determined for each combination of cylinder, cloth and wetting agent.

Because air temperature affects the thermal and physical properties of air consideration was given to curve-fitting of a *Nu*, *Re*, *Pr* correlation. However, the range of air temperatures used during cooling trials was only 0–10°C (*Pr* changes from 0.707 at 0°C to 0.705 at 10°C and *Re* by 6.2% due to changes in viscosity). These changes are small compared with uncertainties in the measurement systems. Given that the two cylinder sizes had to be separately considered because of possible cloth differences, six separate heat transfer coefficient/air velocity best-fit equations (allowing for wetting agent differences) were considered the most accurate way to determine heat transfer coefficients. The best-fit equations to the measured data were:

1. small cylinder, water (9 runs)

$$h = 19.52\ v_a^{0.416} \qquad (R^2 = 0.993) \tag{9}$$

2. small cylinder, NaCl (10 runs)

$$h = 18.09\ v_a^{0.438} \qquad (R^2 = 0.989) \tag{10}$$

3. small cylinder, KCl (9 runs)

$$h = 18.24\ v_a^{0.433} \qquad (R^2 = 0.985) \tag{11}$$

4. large cylinder, water (12 runs)

$$h = 15.55\ v_a^{0.501} \qquad (R^2 = 0.980) \tag{12}$$

5. large cylinder, NaCl (8 runs)

$$h = 15.16\ v_a^{0.457} \qquad (R^2 = 0.992) \tag{13}$$

6. large cylinder, KCl (9 runs)

$$h = 15.48\ v_a^{0.472} \qquad (R^2 = 0.988) \tag{14}$$

The interested reader can find these equations and the data plotted in the source thesis (Chuntranuluck, 1995). The power law exponents of approximately 0.5 are consistent with the measurements of Daudin and Swain (1990) who used a square root relationship to fit measured data for transfer coefficients to cylinders.

Equilibrium temperature analysis

At the equilibrium temperature (T_{eq}), the convective cooling rate and water vaporisation rate are in balance. In Part 1, the equations for the equilibrium temperature were derived using the Lewis relationship (Chuntranuluck *et al.*, 1998a). The apparent steady-state condition at 15 h was used as the experimental measure of T_{eq} because all runs had reached steady state within the sensivity of the measurement system by this time. The measured values, ($T_{eq,exp}$), could be either higher or lower than the mean air temperature, depending on the relative humidity and water activity. The observed differences were as large as 1–2°C. Figure 2 illustrates the case where a_w exceeds H_r.

TABLE 1
Differences Between Results Calculated by the Finite Difference Simulations of Chuntranuluck *et al.* (1998a) and Results from the Experiments (all data)

	% difference in f_{Evap}/f_{Conv}	*% difference in* j_{cEvap}/j_{cConv}	*% difference in time to* Y_c =			*Abs. error in* T_{eq} (°C)
			0.10	*0.35*	*0.70*	
Mean	+2.1	−0.2	−2.2	−2.1	−1.9	0.0
SD	4.1	3.2	4.1	3.6	4.5	0.2
95% conf. interval	−6.2 to +10.5	−6.7 to +6.3	−10.6 to +6.2	−9.5 to +5.3	−11.0 to 7.2	−0.4 to +0.3

Tables 1 and 2 show that the experimental steady state temperature ($T_{eq,exp}$) closely matched the calculated equilibrium temperature ($T_{eq,pred}$, determined using eqn (6) without significant lack of fit. The 95% confidence bounds of differences were −0.4°C to +0.3°C, which is of the same magnitude as the estimated measurement uncertainty. It was concluded that eqn (6) adequately predicted T_{eq}, which in itself implies that the Lewis relationship was an adequate way to model the actual processes, even though the air velocities were as low as 0.5 m s^{-1}, the bottom limit at which Daudin and Swain (1990) found that the Lewis relationship would normally be assumed to hold.

Linearization of semi-log plots

When modified $Y_{c,exp}$ values were calculated using $T_{eq,exp}$ in eqn (1), it was observed that the plots of ln $Y_{c,exp}$ vs *Fo* were successfully linearised. For example, Fig. 3 was derived by replotting the data of Fig. 2. The jagged appearance of the lines at lower $Y_{c,exp}$ arises from both the analogue to digital conversion accuracy in the data

TABLE 2
Differences Between Results Calculated by the Proposed Curve-fitted Algebraic Equations (Simple Model) and Results from the Experiments (all Data)

	% difference in f_{Evap}/f_{Conv}	*% difference in* j_{cEvap}/j_{cConv}	*% difference in time to* Y_c =			*Abs. error in* T_{eq} (°C)
			0.10	*0.35*	*0.70*	
Mean	+1.7	−0.4	−1.7	−1.8	−2.2	0.0
SD	4.0	2.9	4.2	3.8	4.7	0.2
95% conf. interval	−6.5 to +9.9	−6.3 to +5.6	−10.2 to +6.9	−9.6 to +6.0	−11.9 to +7.5	−0.4 to +0.3
R^{2a}	0.944	0.900	0.932	0.890	0.862	— —

[a]Correlation coefficient between (a) % difference between simple method prediction and experiment; and (b) % difference between finite difference predictions and experiments.

logging system and because the temperature difference is approaching the order of magnitude of the accuracy of the thermocouples. The portion of the line below $Y_{c,exp} = 0.70$ could be best-fitted by a straight line with $R^2 > 0.99$ for all runs. This verified that T_{eq} satisfactorily linearised the cooling curves.

Cooling with evaporative effects

In the most extreme cases, the relative rate of cooling with evaporation to convection only in the experiments was about 2 to 1, less than the extreme of 2.9 to 1 found in the theoretical analysis (Chuntranuluck *et al.*, 1998a), and thus reflecting that the experimental ranges were not as wide as the ranges used in method development. Experimental values of f_{cEvap} and j_{cEvap} were derived from plots of ln $Y_{c,exp}$ vs *Fo* described above. These are tabulated in relation to the experimental conditions by Chuntranuluck (1995), and thus can be accessed by the interested reader.

The calculated values of f_{Evap} and j_{cEvap} from the finite difference method, agreed within -6 to $+10\%$ of the experimental data (Table 1). The mean offset for the f values was $+2.1\%$, whereas for the j values the mean error in predicting the experimental values was -0.2%. When the calculated values of f_{Evap} and j_{cEvap} from the simple model were compared with the experimental data, it was found that the

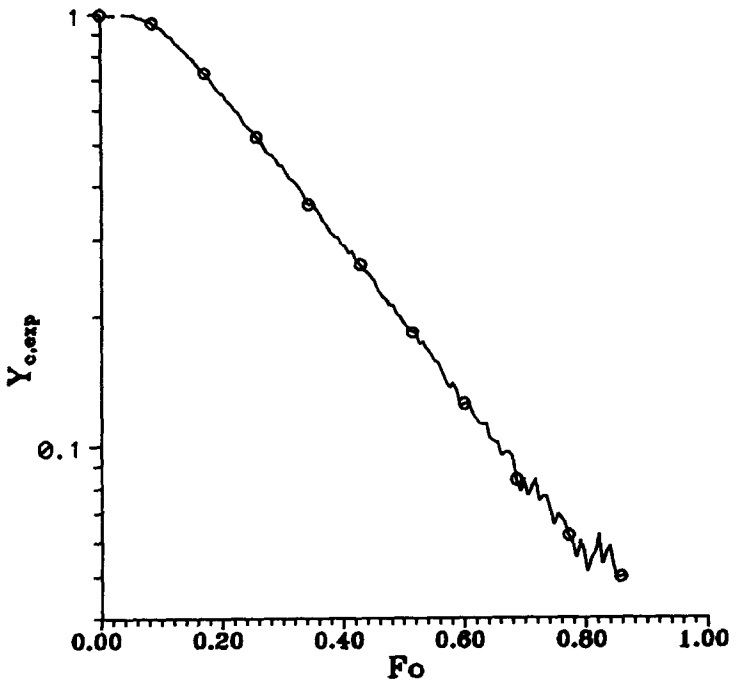

Fig. 3. Plot of ln $Y_{c,exp}$ versus *Fo*, derived using $T_{eq,exp}$ as the reference temperature for calculation of Y values from measured data in Fig. 2.

agreement was within −7 to +10% (Table 2). The mean offset for the f values was +1.7%, and for the j values −0.4%. Relative to the experimental results the finite difference and simple model gave similar predictions.

Overall, the agreement between the simple model and the experimental results was considered acceptable taking into consideration likely data uncertainties, especially in heat transfer coefficients, and the possibility of measurement thermocouples not being positioned exactly at the centre of the products.

Testing for the mass average temperature is difficult, requiring knowledge of the full position–temperature history across the test cylinders. Hence it was not attempted, but it is unlikely that parameters related to centre temperature would be well predicted, and those for mass-average temperature badly predicted.

Chilling time prediction

The major interest of the industrial community is in chilling time prediction. Chilling times to reach certain temperatures ($T_{c,exp}$) which corresponded to $Y_{c,exp} = 0.10$, 0.35, and 0.70 were calculated. The corresponding $Y_{c,pred}$ value at which to make predictions was:

$$Y_{c,pred} = \frac{(T_{c,exp} - T_{eq,pred})}{(T_{in} - T_{eq,pred})} \tag{15}$$

The predicted chilling time (t_{pred}) to reach $T_{c,exp}$ was then found by substituting $Y_{c,pred}$, $j_{cEvap,pred}$ and $f_{cEvap,pred}$ in eqn (7). The results are presented in Table 1 and Table 2. The finite difference and simple model failed to predict experimental data in similar ways, as indicated by the correlation coefficients between % difference of the two models being close to 1.0. The agreements at $Y_{c,exp} = 0.10$ and $Y_{c,exp} = 0.35$ were within about ±10%, and at $Y_{c,exp} = 0.70$ was within about ±11%. The reason for the poorer agreements at $Y_{c,exp} = 0.70$ is that the exponential cooling regime is not always well established before this $Y_{c,exp}$ is reached. This was discussed in Part 1, and is a well-known weakness of any model based on exponential behaviour. The slightly worse agreement at $Y_{c,exp} = 0.10$ compared with $Y_{c,exp} = 0.35$ arises because the former is more influenced by any uncertainty in $T_{eq,exp}$.

To illustrate the overall benefit of the new models, Fig. 4 and Fig. 5 show plots of centre temperatures vs time for the numerical model of Chuntranuluck *et al.* (1998a), with and without evaporation, for the experimental results, and for the simple model. Figure 4 shows one of the more closely predicted runs and Fig. 5 shows a badly predicted run. It can be seen that evaporation makes the cooling rate significantly faster than for convection only, and that the simple model and the finite difference models gave essentially the same results in even the worst case. Overall, confidence in the model is increased by these results, the differences between model and prediction being in part due to experimental uncertainty.

Those wishing to apply the proposed prediction method may wish to consult a full worked example on its use (Chuntranuluck, 1995). In seeking to apply the method it must still be remembered that it has only been derived and tested for the three basic shapes, and for situations where water activity can be assumed to be constant but not necessarily unity. The assumption of constant a_w may not be true for many real food materials. Therefore, in Part 3 (Chuntranuluck *et al.*, 1998b), heuristics for

extending the methodology to real food materials are discussed. These are intended to extend the range of applicability of the methodology.

CONCLUSIONS

The algebraic model proposed in Part 1 for prediction of chilling times where cooling is by evaporation as well as convection at the product surface predicts measured equilibrium temperature, intercept and slope parameters of semi-log unaccomplished temperature change vs time plots as accurately as can reasonably be expected, taking into account data uncertainties. Chilling times are also predicted sufficiently accurately for many industrial applications. The simple model can be used with confidence across the ranges of conditions for which it was derived and tested:

T_a	0–15°C
T_{in}	20–50°C
a_w	0.6–1.0

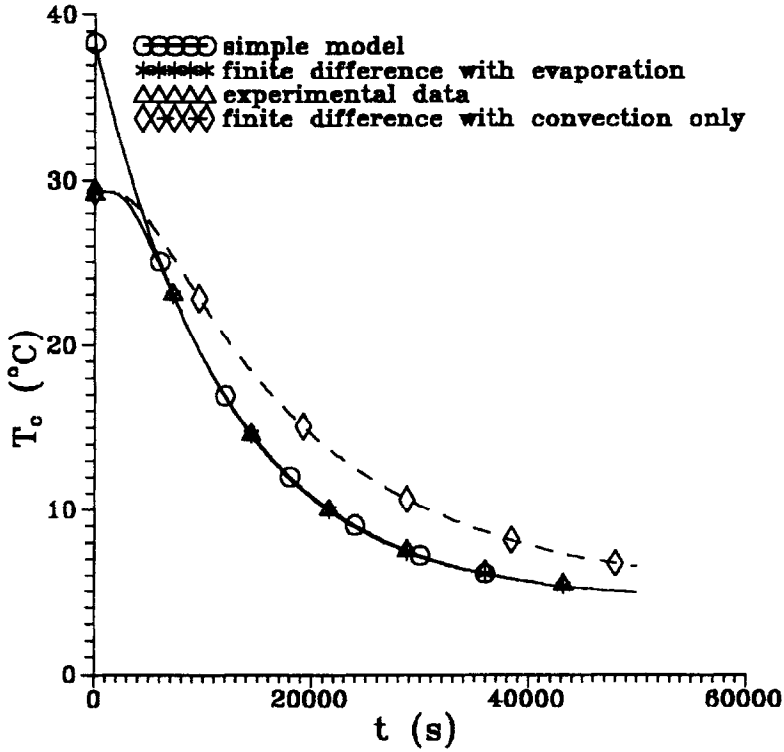

Fig. 4. Plot of sample centre temperature (°C) vs time (s) for a chilling run in which there was excellent agreement between predictions by both finite difference and proposed simple methods and experimental data.

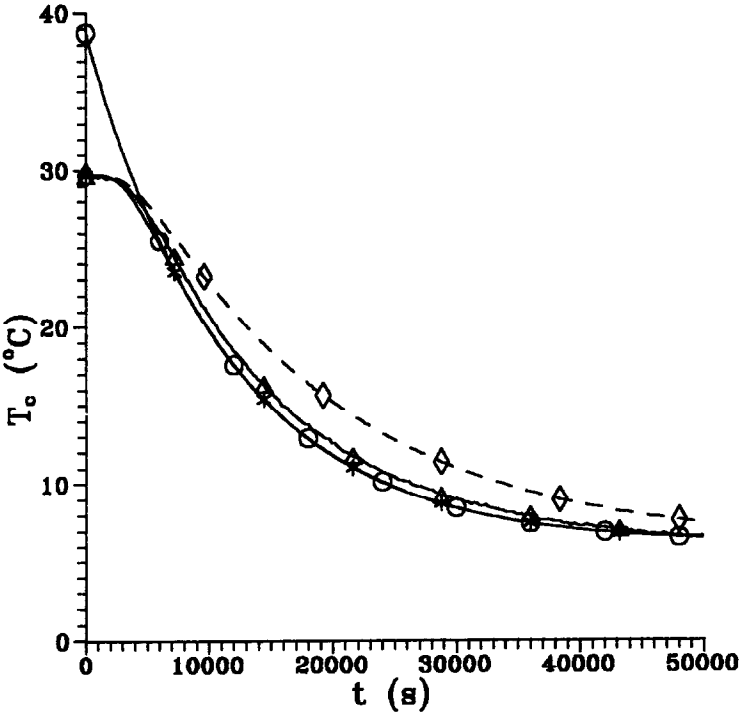

Fig. 5. Plot of sample centre temperature (°C) vs time (s) for a chilling run in which there was poor agreement between predictions by both finite difference and proposed simple methods and experimental data. Key as in Fig. 4.

H_R	0.5–1.0
Bi	0.1–10
Shape	infinite slab, infinite cylinder, sphere

This range covers most conditions likely to be encountered in industrial chilling situations. Further research to improve the representation of the water activity of the product less simplistically than a constant, but non-unity value, is justified. This aspect is addressed in Part 3.

REFERENCES

Chuntranuluck, S. (1995). Prediction of chilling times of foods subject to both convective and evaporative cooling at the product surface. PhD thesis, Massey University, North Palmerston, New Zealand.

Chuntranuluck, S., Wells, C. M. & Cleland, A. C. (1998a). Prediction of chilling times of foods in situations where evaporative cooling is significant—Part 1. Model development. *J. Food Engng*, **37**, 111–125.

Chuntranuluck, S., Wells, C. M. & Cleland, A. C. (1998b). Prediction of chilling times of foods in situations where evaporative cooling is significant—Part 3. Applications. *J. Food Engng*, **37**, 143–157.

Cleland, A. C. (1990). *Food Refrigeration Processes: Analysis, Design and Simulation*. Elsevier, London.

Cleland, D. J., Cleland, A. C. & Jones, R. S. (1994). Collection of accurate experimental data for testing the performance of simple methods for food freezing time prediction. *J. Food Proc. Eng.*, **17**, 93–119.

Daudin, J. D. & Swain, M. V. L. (1990). Heat and mass transfer in chilling and storage of meat. *J. Food Engng*, **12**, 95–115.

Riedel, L. (1960). Eine prufsunstanz fur gefrierversuche. *Kaltetechnik*, **12**, 222–226.